Nuclear Materials and Energy 15 (2018) 254–260

Contents lists available at ScienceDirect

Nuclear Materials and Energy

journal homepage: www.elsevier.com/locate/nme

An F82H steel pressurized tube creep capsule for irradiation in HFIR☆

Padhraic L. Mulligan[a,*], Hideo Sakasegawa[a,b], Hiroyasu Tanigawa[b], Christian M. Petrie[a], Joel L. McDuffee[a], Yutai Katoh[a]

[a] Oak Ridge National Laboratory, Oak Ridge, TN 37831 USA
[b] National Institutes for Quantum and Radiological Science and Technology (QST), Rokkasho, Aomori 039-3212, Japan

ARTICLE INFO

Keywords:
Pressurized tube
Irradiation creep
F82H IEA heat
HFIR

ABSTRACT

A novel capsule design has been developed for measurement of irradiation creep in pressurized tubes and is being used to irradiate reduced activation ferritic/martensitic F82H steel creep test specimens. These tests are being conducted in the flux trap of the High Flux Isotope Reactor at the Oak Ridge National Laboratory. The capsule design uses a tight-fitting corrugated aluminum foil placed in the center of a vanadium alloy holder to conduct heat from the centrally located test specimen. The foil acts as a compressible thermal interface between the pressurized tube and holder, maintaining a constant thermal resistance (and thus a constant tube temperature gradient) during irradiation, regardless of differential thermal expansion, creep, and swelling in the test specimen. Mechanical interference with creep deformation of the specimen tube is minimized by using a thin (0.05 mm) foil with sufficient room to crush. Finite element analysis of the contact pressure between the specimen and foil, combined with thermal creep in the foil, showed little interference with specimen stress conditions. Specimens were designed to experience hoop stresses of 380, 300, 150, and 0 MPa at a temperature of 300 °C while being irradiated to a dose of 3.7 dpa. Passive SiC thermometry is located within the pressurized tube and the holder material for confirmation of experiment irradiation target temperatures. This work discusses aspects of the capsule's fabrication and design, including thermal models of the capsule during irradiation.

1. Introduction

Various materials for fusion blanket structural applications have been selected for their preferable thermophysical properties, low activation, and reduced swelling characteristics. While these traits are desirable, irradiation creep is among the most important design-limiting phenomena for structural materials in nuclear applications. For many of these materials, the database of irradiation creep rates is sparse and in need of experimental measurement. This article describes the design of a novel capsule that will produce necessary irradiation creep performance data while reducing the cost and effort required for current post-irradiation specimen recovery.

Historically, irradiation creep measurements have relied on diametrical measurements of thin-walled pressurized tubes pre- and post-irradiation. Pressurized tubes (PTs) are composed of the material under consideration and are internally pressurized to generate circumferential hoop stress in the outer wall. This has been a preferred experimental format for several reasons [1]: (a) the smaller test volume minimizes gradients in neutron dose and temperature, (b) the reduced mass lowers material activation for post irradiation examination (PIE), (c) stress is applied without external mechanical connections to reactor components, and (d) stress is nearly constant for large creep-induced strains (≤ 20%) since reduction in gas pressure is offset by thinning of the tube wall.

PTs are also versatile in their range of experimental conditions, with some studies generating hoop stresses of 470 MPa [2], neutron radiation damage of 208 dpa [3], and temperatures of 750 °C [4,5]. Specimen temperatures are typically regulated by immersing the PTs in a molten bath of lithium [6–9], sodium [3,10–12], or NaK [2]. Liquid metal/salt immersion of PTs has been the primary means of temperature control as this technique maintains specimen temperature despite deformation caused by thermal expansion, irradiation creep, and swelling without imposing resistive mechanical stress that may bias creep performance data. However, cleaning and extracting PTs from solidified baths following irradiation can be expensive, challenging, and generate large amounts of radioactive waste. PT specimens have also

* Corresponding author.
E-mail address: mulliganpl@ornl.gov (P.L. Mulligan).

https://doi.org/10.1016/j.nme.2018.05.011
Received 15 December 2017; Received in revised form 6 May 2018; Accepted 15 May 2018
Available online 24 May 2018

been gas-bonded to their irradiation capsules [13], but this generally requires the use of expensive instrumentation and active temperature monitoring.

This work details a novel irradiation capsule for PTs, which uses a thin, crushable, corrugated 1100 aluminum foil to maintain thermal contact with the specimen during circumferential expansion, eliminating the need for a liquid metal/salt bath to regulate temperature. Quantification of creep in the PTs is performed by measuring the diametrical expansion via laser profilometry in post irradiation examination (PIE). This design leverages previous work using an embossed aluminum foil for an irradiation experiment examining high heat flux in SiC/SiC composite tubes [14]. The assembly fits within a standard, passively controlled, High Flux Isotope Reactor (HFIR) irradiation "rabbit" capsule, allowing the creep experiment to take place in the flux trap at a higher and harder neutron flux. This compact design also gives more reliability over steady state specimen temperature, as the tube's precise axial position in the core is known, permitting temperature control by optimizing the size of insulating gas gaps between the capsule's internal components. Additionally, the lack of a liquid bath reduces the cost and level of effort needed in PIE specimen recovery. This experimental format is also significantly less expensive than large instrumented experiments previously conducted for PT irradiation creep studies, as it does not require active temperature control. However, this design only permits a single PT specimen in each irradiation capsule.

This new capsule design was used to construct four reduced activation ferritic/martensitic (RAFM) F82H, IEA heat, PT test specimens pressurized over a range of hoops stress conditions. Stresses were selected to replicate conditions studied previously [13] with this material to compare strain rates and verify that the embossed foil has negligible impact on material creep. By validating this design, future irradiation creep studies using PTs can be performed at low cost. Competed capsules were inserted into the HFIR flux trap for two cycles of irradiation, beginning with cycle 475.

2. Material and methods

2.1. Experiment design

Endcaps and thin-walled tube sections for assembling PTs were machined from F82H, IEA heat, with chemical compositions given in Table 1. The PT walls (Fig. 1, Table 2) were fabricated to a 25.4 mm length, 4.57 mm outer diameter, and 0.25 mm wall thickness, for a geometry commensurable with other pressurized tube studies [1,3,6–8,13]. One endcap for each PT included a 0.2 mm hole for fill gas pressurization. β-phase SiC ($\rho = 3.21\ g/cm^3$), grown via chemical vapor deposition (CVD), was machined into tubes and placed in each PT for peak irradiation temperature measurement (Fig. 2). The SiC thermometry served as an internal passive temperature monitor, as well as a safety mechanism to reduce free volume within the PT and prevent over-pressurization of the aluminum housing in the event of a PT rupture. Electron beam welding in vacuum was used to join the endcaps to the tube, with the SiC thermometry placed inside. A subsequent post-weld heat treatment was performed for 1 hour at 720 °C in vacuum, with each tube wrapped in a tantalum foil for impurity gettering. The tubes were then pressurized with ultra-high purity (99.999%) helium in a high pressure chamber and sealed using a 400 W pulsed Nd:YAG laser through a quartz window. Laser profilometry was repeated four times over the central $^3/_5$ axial length of each PT before and after pressurization to determine the average diameter of each specimen. Internal pressures in the four tubes were chosen to generate circumferential hoop stresses of 0, 150, 300, and 380 MPa at a 300 °C irradiation temperature. All PT specimens were helium leak checked prior to irradiation to ensure a hermetic seal.

Table 1
Chemical composition of F82H, IEA heat steel.

Element	wt%	Element	wt%
Cr	7.85	N	0.007
W	1.98	Ti	0.004
V	0.19	P	0.003
Mn	0.10	Mo	0.0028
C	0.09	Co	0.0026
Si	0.07	S	0.001
Ta	0.04	B	0.0002
Ni	0.02	Nb	0.0002
Cu	0.01		

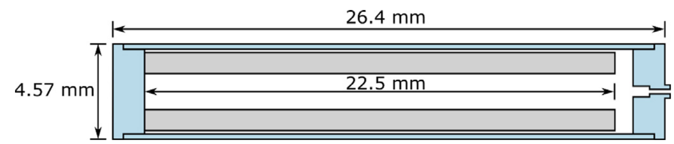

Fig. 1. Schematic of PT specimen with internal SiC thermometry.

Table 2
Nominal dimensions and materials of primary capsule components.

Component	Material	Dimension	Nominal value (mm)
Internal thermometry	SiC	Inner diameter	1.85
		Outer diameter	3.85
PT wall	F82H	Inner diameter	4.06
		Outer diameter	4.57
Embossed foil	Al 1100	Thickness	0.05
Holder	V-4Cr4Ti	Inner diameter	5.02
		Outer diameter	9.37
Holder thermometry	SiC	Length	25.0
		Width	0.50
		Thickness	0.25
Housing	Al 6061	Inner diameter	9.52
		Outer diameter	10.97

A thin (0.05 mm) sinusoidally embossed aluminum foil surrounds the PT, with a 0.25 mm peak to peak height, allowing sufficient space for the tube to expand without causing mechanical interference. The foil and PT were assembled and inserted into the center of a V-4Cr-4Ti holder which was designed to control specimen temperature through an optimized radial gas gap between the holder and the aluminum housing (Fig. 3). Only one PT was assembled in an irradiation capsule to prevent over pressurization of the aluminum housing, should the PT rupture. V-4Cr-4Ti was chosen as the holder material for its lower thermal expansion coefficient relative to the PT material. This ensures stable thermal contact between the centrally located PT, corrugated foil, and holder. Two β-phase SiC rectangular bar specimens were placed into channels in the V-4Cr4-Ti holder for additional temperature indication. The holder was centered axially in the aluminum capsule using two titanium springs, and was centered radially using centering thimbles located at ends of the holder assembly. The aluminum housing was then welded to an endcap, backfilled with ultra-high purity helium for heat transfer, and seal welded for irradiation.

2.2. Experimental irradiation facility

Assembled capsules were loaded into the central flux trap of the HFIR for two cycles of irradiation. HFIR is a pressurized, light-water moderated and cooled research reactor at the Oak Ridge National Laboratory, operating at 85 MW thermal power with an average cycle length of 24–25 days [15]. Within the flux trap, there are three facilities available for capsule irradiation: peripheral target positions, target rod rabbit holder (TRRH) positions, and hydraulic tube positions. TRRH positions can accommodate up to seven capsules stacked vertically, with the fourth capsule positioned at the core horizontal midplane. The capsules discussed in this work were placed in TRRH positions 3 and 5,

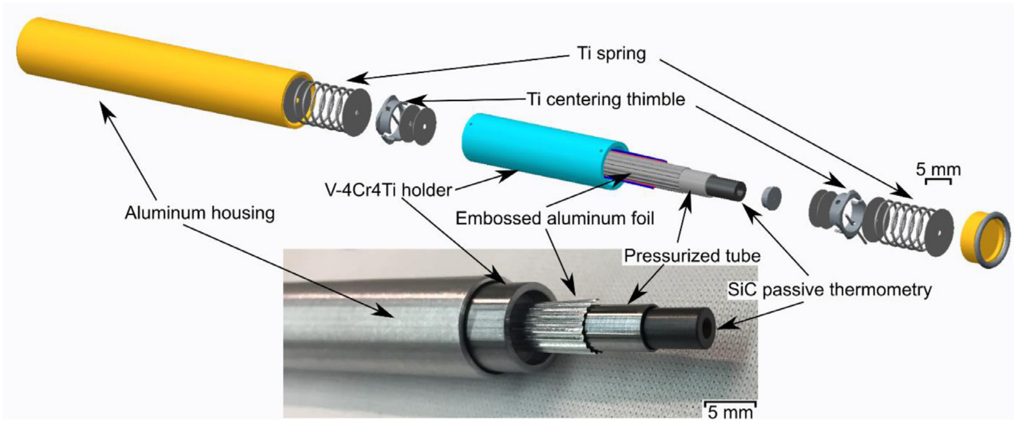

Fig. 2. CAD model and picture of irradiation capsule with primary components labeled.

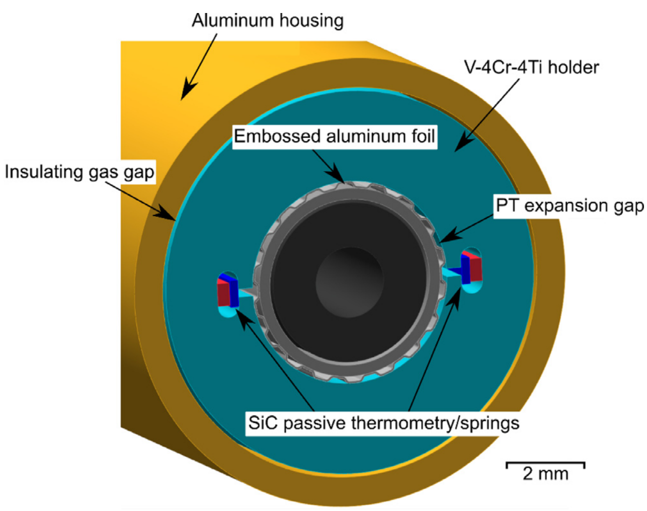

Fig. 3. Section view of capsule midplane showing PT expansion gap, location of SiC passive thermometry, and holder/housing insulating gas gap.

Table 3
HFIR core horizontal midplane heat generation rates for TRRH position.

Material	Peak heat generation rate (W/g)
F82H Steel	39.3
Aluminum	32.5
SiC	32.9
V-4Cr4Ti	46.8
Ti	35.2

slightly below and above the core midplane, respectively. Neutron flux and heat generation rates for these two positions are symmetric about the core horizontal midplane and have an integral average of 95.2% peak power over the length of the irradiation capsule. Calculated peak heat generation rates for the primary materials used in the fabrication of this PT irradiation capsule are listed in Table 3.

2.3. Finite element thermal/structural modeling

Thermal and structural modeling of the capsule design was performed using the ANSYS finite element software package. 3D computer aided design (CAD) models of the irradiation capsule were produced and imported into ANSYS to determine the gas gaps necessary to achieve PT design temperatures. The efficacy of the embossed aluminum foil was also analyzed, and passive thermometry temperatures were ascertained to compare with PIE results. Rather than meshing gas gaps, custom solution methods were used to determine the thermal contact conductance between parts in contact or in close proximity to each other [16]. Neutronics and activation calculations performed by researchers at Oak Ridge National Laboratory were used to determine neutron, photon, and decay heat generation rates in each material to supply heat source terms for the ANSYS model (Table 3). The convective heat transfer coefficient and coolant temperature were also previously calculated parameters; thereby providing boundary conditions for the model.

Irradiation capsules were initially modeled in 2D (Fig. 4) at the capsule midplane employing 90-degree symmetry. The insulating gas gap was adjusted after each solution convergence until the average PT wall temperature reached the 300 °C design temperature. Capsule component temperatures and linear heat loads calculated by ANSYS were recorded and used to calculate the contact conductance through the embossed foil using the following equations:

$$C = \frac{q''}{T_{tube} - T_{holder}} \tag{1}$$

$$q'' = \frac{q'_{thermometry} + q'_{tube}}{2\pi r_{tube}} \tag{2}$$

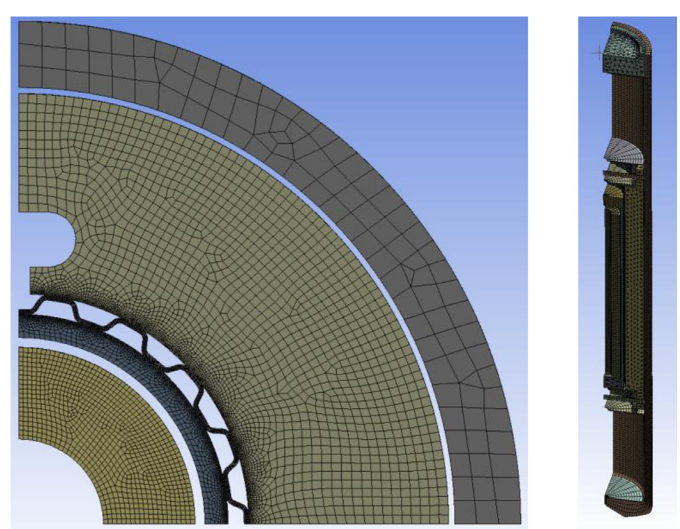

Fig. 4. Meshed 2D (left) and 3D (right) model of the PT capsule assembly.

where:

C = Contact conductance through foil $(W/m^2 \cdot K)$
q'' = Heat flux at PT outer surface (W/m^2)
T_{tube} = Temperature of PT outer surface $(^\circ C)$
T_{holder} = Temperature of holder inner surface $(^\circ C)$
q_i' = Linear heat generated in component i (W/m)
r_{tube} = Outer radius of PT (m)

The foil contact conductance was then applied to the PT/holder interface in a 3D meshed, 90-degree symmetry model with the foil suppressed. This simplification reduced meshing complexity in the foil region, and produced a more robust and efficient model. Simulations were then performed to (a) determine temperature profiles in the PT specimen and capsule components, (b) select the appropriate holder/housing gas gap, and (c) determine the sensitivity of the SiC thermometry inside the PT with respect to repositioning and PT diametrical expansion. While there are several axial positions available for capsule irradiation in the HFIR flux trap, the reported results are for capsules located at the HFIR core midplane (TRRH-4), where neutron flux and heat generation rates are greatest.

3. Results and discussion

3.1. 2D simulation results

Temperature contour plots from the 2D ANSYS simulation are shown in Fig. 5. Temperature summaries of the primary capsule component are found in Table 4. The PT wall showed a minor variation in temperature, with lower temperatures occurring at locations in contact with the embossed foil. However, all PT temperatures varied by only 2 °C. Temperatures and heat load data used to calculate the embossed foil contact conductance are summarized in Table 5.

Mechanical constraint of PT expansion due to the embossed foil was analyzed by determining the contact pressure between the embossed foil and PT wall in 2D ANSYS simulations. Results showed an average contact pressure of 2.25 MPa before accounting for tube expansion due to creep. This contact pressure has a net effect of reducing radial pressure on the tube wall and corresponds to a 13% reduction in PT wall hoop stress for the 150 MPa tube, 6.6% reduction for the 300 MPa tube, and 5.0% reduction for the 380 MPa tube. However, the embossed 1100 aluminum foil will be at an average temperature of 287 °C, nearly 45% of the material melting point. At this elevated temperature, stress in the foil will be reduced through thermal creep, resulting in lower contact pressures, reduced mechanical interference, and negligible changes to applied hoop stress in the PT.

Table 4
2D finite element model temperatures [average (min–max)].

Component	Temperature (°C)
SiC PT thermometry	337 (336–337)
PT wall	300 (299–300)
Embossed foil	287 (286–289)
Holder	259 (244–273)
Housing	64 (63–65)

Table 5
Parameters used to calculate contact conductance through the embossed foil.

Parameter	Value
$q'_{thermometry}$	931.2 W/m
q'_{tube}	1,049.5 W/m
r_{tube}	0.002285 m
q''	137,960 W/m^2
T_{tube}	299 °C
T_{holder}	273 °C
C	5,306 (W/m^2-K)

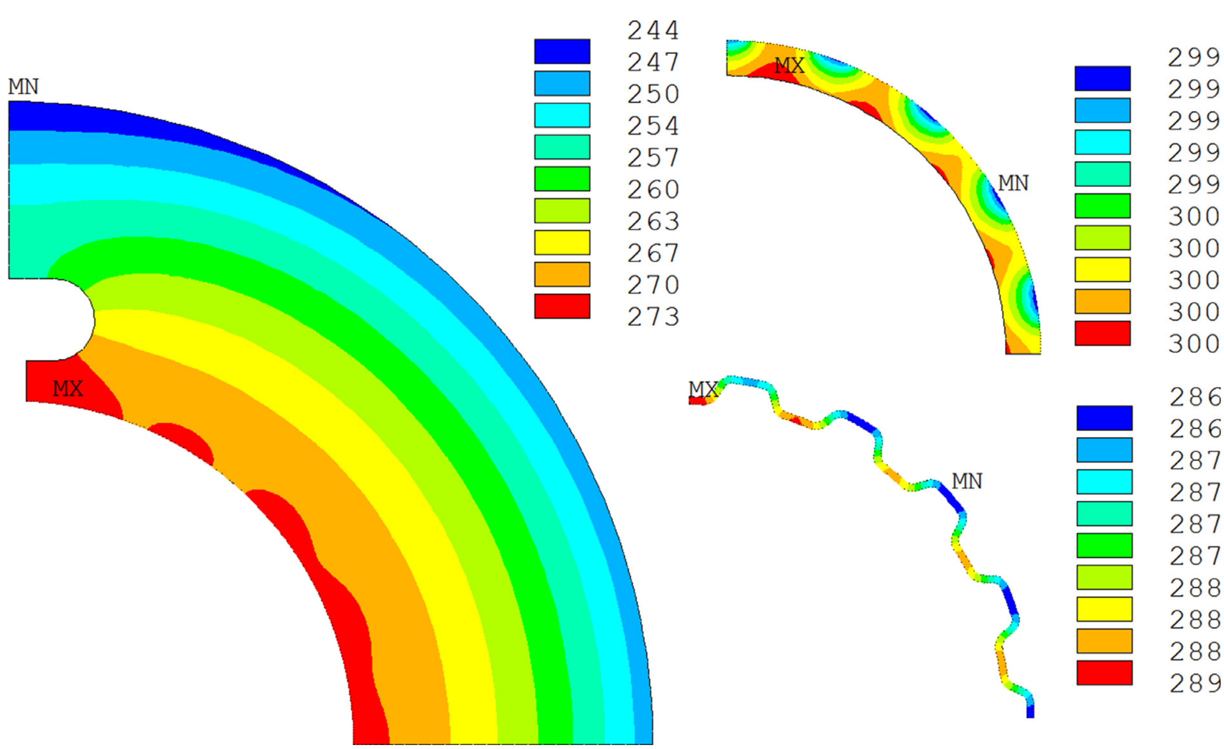

Fig. 5. Select temperature contour plots (°C) for 2D simulations. Results are shown for V-4Cr-4Ti holder (left), PT wall (top right), and embossed foil (bottom right).

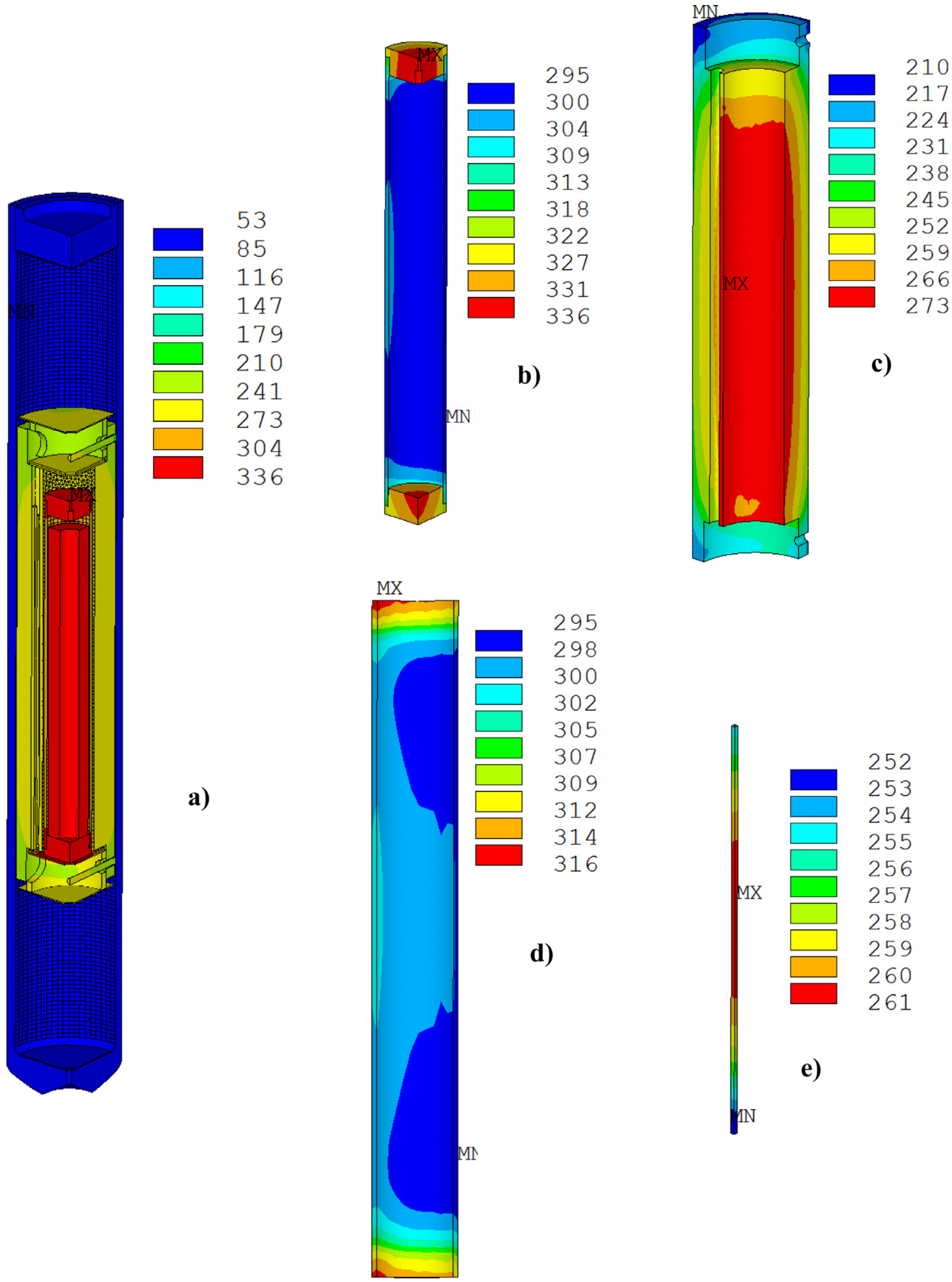

Fig. 6. Temperature (°C) contour plots from 3D ANSYS simulations at reactor midplane position for all capsule components (a), PT (b), holder (c), PT with endcaps suppressed (d), and holder thermometry (e).

Table 6
3D PT capsule component temperatures [average (min-max)] at HFIR midplane location (TRRH-4).

Component	Temperature (°C)
Housing	59 (53–65)
Housing end cap	69 (67–70)
Holder	254 (210–273)
Centering thimbles	238 (191–269)
PT wall	299 (295–316)
PT end caps	329 (319–336)
Inner SiC	334 (332–335)
Holder SiC	258 (252–261)

3.2. 3D simulation results

A 3D analysis of the capsule was performed to determine component temperatures, which used the foil contact conductance calculated in the 2D simulation. This approach simplifies the 3D model from a computation complexity standpoint by removing the complicated foil geometry and significantly reducing the number of elements needed to represent the foil. Fig. 6 shows temperature contour plots obtained from these simulations. Only a 5 °C variation in PT wall temperature was observed over the central ~80% of the axial length, with the greatest temperature increase occurring at the ends of the tube. This end effect was caused by the endcaps, which are relatively more massive than the

Table 7
Temperature (°C) [average (min-max)] summary of various SiC thermometry orientations in PT.

	PT/thermometry case considered		
Component	Tube bowed (Case 1)	SiC centered (Case 2)	SiC contact (Case 3)
Inner SiC	340 (336–341)	334 (332–335)	323 (320–324)
PT wall	299 (295–317)	299 (295–316)	299 (288–318)

PT and create a higher heat load. The uniform temperature profile over the diametrically characterized region of the PT (central $^3/_5$ of PT length) demonstrates that the embossed foil is a suitable experimental format for PT irradiation creep experiments. Table 6 summarizes the primary component temperatures for this 3D analysis.

3.3. PT SiC thermometry sensitivity

SiC passive thermometry specimens were placed in the holder T-slots along with SiC leaf springs to maintain physical contact with the holder material, giving a reliable heat transfer path and an accurate indication of holder temperature. The SiC thermometry inside the PT is freestanding, giving radial and axial gaps for thermal expansion and irradiation induced swelling in the SiC, and eliminating the possibility of additional stress imposed on the PT. To determine the temperature sensitivity of the freestanding internal thermometry, an analysis was performed by comparing the temperature profiles in three scenarios: (1) the PT bulged in the center by 1.5% of the original diameter, (2) cylindrical thermometry centered in the tube, and (3) thermometry in contact with a wall of the tube. For each scenario, a summary of inner SiC thermometry and PT temperatures can be seen in Table 7, and temperature profiles for the thermometry are shown in Fig. 7. In each case, temperatures in the PT wall were nearly unaffected, while average temperatures in the thermometry had a maximum variation of 17 °C. Knowledge of this temperature variability will be useful when verifying PT irradiation temperatures through SiC dilatometry post-irradiation [17].

4. Conclusions

A novel capsule design was analyzed to provide irradiation creep data from pressurized test capsules made from the RAFM steel F82H, IEA heat. This design allows for irradiation to occur at a virtually uniform specimen temperature without the use of a liquid metal/salt bath; reducing the cost of PIE and permitting in-core irradiation in HFIR. Instead, an embossed 1100 aluminum foil was used to provide a crushable heat transfer link between the specimen and capsule holder. This foil has minimal impact on the PT specimen stress condition due to the high temperature relative to the foil's melting point, and low contact pressure with the specimen relative to the internal pressure of the PT. The results shown in this work demonstrate that the temperature profiles and design parameters specific to F82H PT irradiation capsules meet the target temperature of 300 °C. Four capsules were assembled using this design with hoop stresses of 0, 150, 300, and 380 MPa, with an expected neutron dose of 3.7 dpa. Laser profilometry of the test specimens was performed before and after pressurization and will be repeated after two HFIR cycles for quantitative creep measurements. Results of this PT creep study will be compared to previous studies of the same material to determine the efficacy of this design. Post-irradiation profilometry is expected to occur in early 2018.

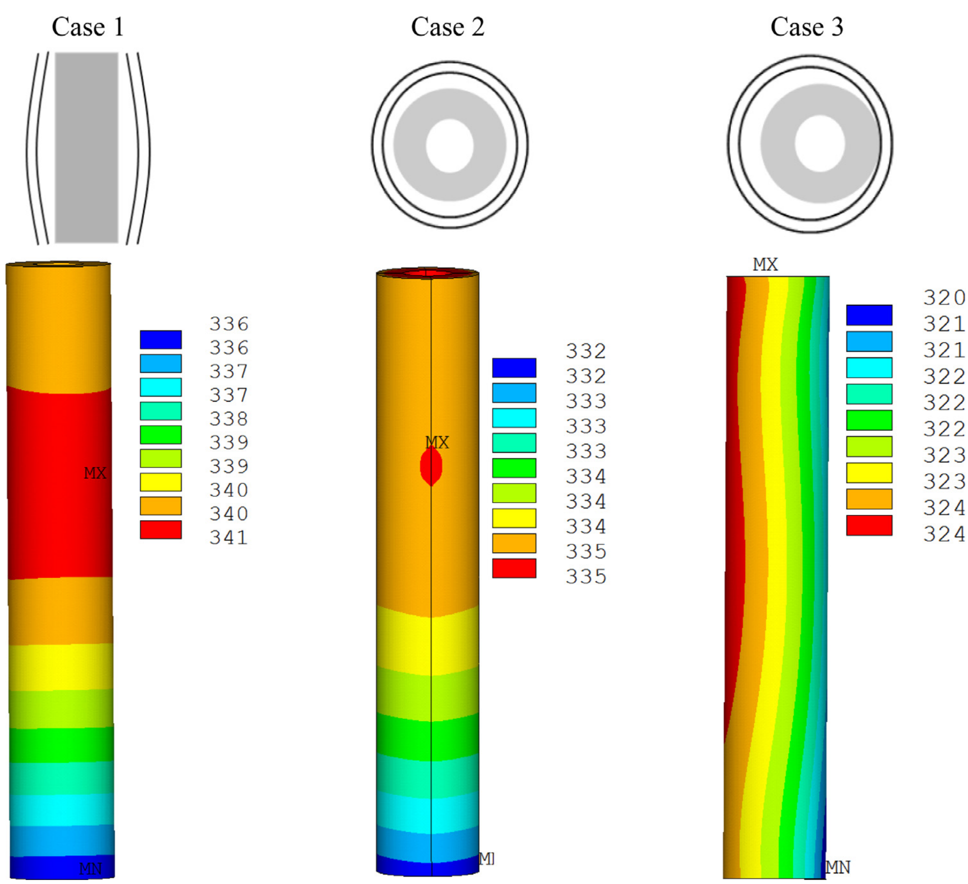

Fig. 7. Temperature (°C) profile of inner SiC thermometry in three scenarios: (1) PT walls bowed axially to 1.5% the original diameter, (2) thermometry centered in PT (middle), and (3) thermometry in tangential contact with one wall of PT (right). Simplified and exaggerated diagrams of each scenario are located above the temperature profiles.

Acknowledgements

This material is based upon work supported by the US Department of Energy, Office of Science, Office of Fusion Energy Sciences under contract number DE-AC05-00OR22725, and QST of Japan, SPP contract NFE-17-06547.

Supplementary materials

Supplementary material associated with this article can be found, in the online version, at doi:10.1016/j.nme.2018.05.011.

References

[1] F.A. Garner, M.L. Hamilton, R.J. Puigh, C.R. Eiholzer, D.R. Duncan, M.B. Toloczko, A.S. Kumar, The influence of specimen size on measurement of thermal or irradiation creep in pressurized tubes, in: A.S. Kumar, D.S. Gelles, R.K. Nanstad, E.A. Little (Eds.), Effects of Radiation on Materials: 16th International Symposium. ASTM STP 1175 American Society for Testing and Materials, 1993, pp. 631–645.

[2] M.L. Grossbeck, J.A. Horak, Irradiation creep in type 316 stainless steel and US PCA with fusion reactor He/dpa levels, J. Nucl. Mater. 155-157 (1988) 1001–1005.

[3] M.B. Toloczko, F.A. Garner, C.R. Eiholzer, Irradiation creep and swelling of the US fusion heats of HT9 and 9Cr-1Mo to 208 dpa at ∼ 400 °C, J. Nucl. Mater. 212-215 (1994) 604–607.

[4] R.J. Puigh, The in-reactor deformation of the PCA alloy, J. Nucl. Mater. 141-143 (1986) 954–959.

[5] F.A. Garner, R.J. Puigh, Irradiation creep and swelling of the fusion heats of PCA, HT9 and 9Cr-1Mo irradiated to high neutron fluence, J. Nucl. Mater. 179-181 (1991) 577–580.

[6] M. Li, D.T. Hoelzer, M.L. Grossbeck, A.F. Rowcliffe, S.J. Zinkle, R.J. Kurtz, Irradiation creep of the US Heat 832665 of V-4Cr-4Ti, J. Nucl. Mater. 386 (2009) 618–621.

[7] H. Tsai, T.S. Bray, H. Matsui, M.L. Grossbeck, K. Fukumoto, J. Gazda, M.C. Billone, D.L. Smith, Effects of low-temperature neutron irradiation on mechanical properties of vanadium-base alloy, J. Nucl. Mater. 283-287 (2000) 362–366.

[8] H. Tsai, H. Matsui, M.C. Billone, R.V. Strain, D.L. Smith, Irradiation creep of vanadium-base alloys, J. Nucl. Mater. 258-263 (1998) 1471–1475.

[9] D.S. Gelles, Microstructural examination of irradiated and unirradiated V-4Cr-4Ti pressurized creep tube, J. Nucl. Mater. 307-311 (2002) 393–397.

[10] J.M. Vitek, D.N. Braski, J.A. Horak, Effect of preinjected helium on the response of V-20Ti pressurized tubes to neutron irradiation, J. Nucl. Mater. 141-143 (1986) 982–986.

[11] A. Hishinuma, J.M. Vitek, J.A. Horak, E.E. Bloom, Effect of preinjected helium on swelling and microstructure of neutron irradiated pressurized tubes of type 316 stainless steel, in: H.R. Brager, J.S. Perrin (Eds.), Effects of Radiation on Materials: Eleventh Conference. ASTM STP 782, American Society for Testing and Materials, 1982, pp. 92–107.

[12] R.J. Puigh, F.A. Garner, Irradiation creep behavior of the fusion heats of HT9 and modified 9Cr-1Mo steels, in: N.H. Packan, R.E. Stoller, A.S. Kumar (Eds.), Effects of Radiation on Materials: 14th International Symposium (Volume II), ASTM STP 1046 American Society for Testing and Materials, 1990, pp. 527–536.

[13] M. Ando, M. Li, H. Tanigawa, M.L. Grossbeck, S. Kim, T. Sawai, K. Shiba, Y. Kohno, A. Kohyama, Creep behavior of reduced activation ferritic/martensitic steels irradiated at 573 and 773K up to 5 dpa, J. Nucl. Mater. 367-370 (2007) 122–126.

[14] C.M. Petrie, T. Koyanagi, J.L. McDuffee, C.P. Deck, Y. Katoh, K.A. Terrani, Experimental design and analysis for irradiation of SiC/SiC composite tubes under a prototypic high heat flux, J. Nucl. Mater. (2017) 491.

[15] N. Xoubi, R.T. Primm III, Modeling of the High Flux Isotope Reactor Cycle 400, Oak Ridge National Laboratory, Oak Ridge, TN, 2004.

[16] J.L. McDuffee, Heat transfer through small moveable gas gaps in a multi-body system using the ANSYS finite element software, ASME Summer Heat Transfer Conference, Minneapolis, MN, United States, 2013.

[17] A.A. Campbell, W.D. Porter, Y. Katoh, L.L. Snead, Method for analyzing passive silicon carbide thermometry with a continuous dilatometer to determine irradiation temperature, Nucl. Instrum. Meth. B 370 (2016) 49–58.